A coherent all-electrical interface between polar molecules and mesoscopic superconducting resonators

A. ANDRÉ[1,2], D. DEMILLE[3], J. M. DOYLE[2], M. D. LUKIN[2]*, S. E. MAXWELL[2], P. RABL[4], R. J. SCHOELKOPF[1,3] AND P. ZOLLER[4,5]

[1]Department of Applied Physics, Yale University, New Haven, Connecticut 06520, USA
[2]Department of Physics, Harvard University, Cambridge, Massachusetts 02138, USA
[3]Department of Physics, Yale University, New Haven, Connecticut 06520, USA
[4]Institute for Theoretical Physics, University of Innsbruck, Technikerstrasse 25, A-6020 Innsbruck, Austria
[5]Institute for Quantum Optics and Quantum Information of the Austrian Academy of Sciences, A-6020 Innsbruck, Austria
*e-mail: lukin@physics.harvard.edu

Published online: 27 August 2006; doi:10.1038/nphys386

Building a scalable quantum processor requires coherent control and preservation of quantum coherence in a large-scale quantum system. Mesoscopic solid-state systems such as Josephson junctions and quantum dots feature robust control techniques using local electrical signals and self-evident scaling; however, in general the quantum states decohere rapidly. In contrast, quantum optical systems based on trapped ions and neutral atoms exhibit much better coherence properties, but their miniaturization and integration with electrical circuits remains a challenge. Here we describe methods for the integration of a single-particle system—an isolated polar molecule—with mesoscopic solid-state devices in a way that produces robust, coherent, quantum-level control. Our setup provides a scalable cavity-QED-type quantum computer architecture, where entanglement of distant qubits stored in long-lived rotational molecular states is achieved via exchange of microwave photons.

Polar molecules[1] have exceptional features for use in quantum information systems. Stable internal states of polar molecules can be controlled by electrostatic fields, in analogy with quantum dots and superconducting qubits[2–5]. This controllability of polar molecules is due to their rotational degree of freedom in combination with the asymmetry of their structure (absent in atoms). By applying moderate laboratory electric fields, rotational states with transition frequencies in the microwave range are mixed, and the molecules acquire large dipole moments (of the order of a few Debye, similar to the transition dipole moments of optical atomic transitions). These dipole moments are the key property that makes polar molecules effective qubits in a quantum processing system. Furthermore, the application of electric field gradients leads to large mechanical forces, allowing trapping of the molecules. Finally, polar molecules also combine the large-scale preparation available for neutral atoms[6,7] with the ability to move them with electric fields, as with ions[8–10].

Here we show that trapping the molecules at short distances from a superconducting transmission line resonator greatly enhances the coupling of the molecular rotational transitions to microwave radiation, leading to methods both for cooling the molecule and for manipulation of the molecule as a qubit. The qubit can be encoded in rotational states and coherently transferred to the resonator. Although it has already been shown that the free-space dipole–dipole coupling of polar molecules is viable for carrying out quantum operations[11], and that on-chip striplines can be effective for long-range coupling[12], the present work demonstrates for the first time the feasibility of a complete, potentially scalable molecular quantum processor. Key elements include the integration of techniques for molecular trapping and high-fidelity quantum gates at a distance as well as cooling, high-fidelity readout and scalable architecture.

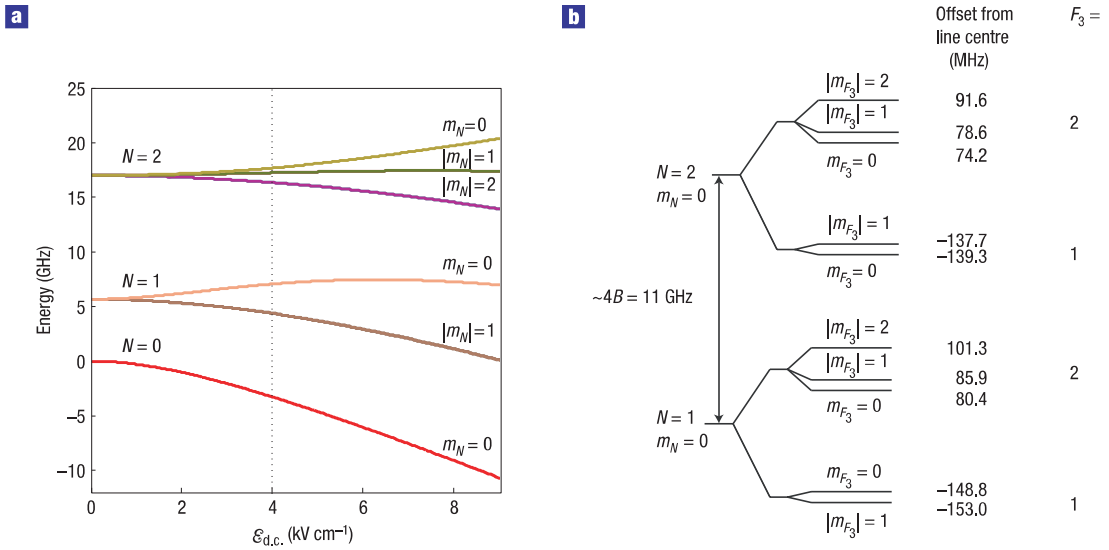

Figure 1 The structure of selected rotational states of CaBr in an electric field. Molecular structure and level shifts of CaBr relevant to the proposed schemes. **a**, Stark shifts of rotational levels in an applied electric field, showing the trappable states $|1\rangle \equiv |N=1, m_N=0\rangle$ and $|2\rangle \equiv |N=2, m_N=0\rangle$ (weak-field seekers). The dotted line marks the field value $\mathcal{E}_{d.c.} = \mathcal{E}_{d.c.}^{off,sweet}$ for which the effective dipole moments of the weak-field-seeking states are the same. **b**, Spin-rotation and hyperfine structure of $Ca^{79}Br$ in a strong electric field. The energies shown are for $\mathcal{E}_{d.c.} = \mathcal{E}_{d.c.}^{off,sweet} = 4\,kV\,cm^{-1}$. The effects of electron and nuclear spin are determined by the spin-rotation hamiltonian[46] $H_{spin-rot} = \gamma_{sr}\mathbf{N}\cdot\mathbf{S}$ and the hyperfine hamiltonian $H_{hfs} = b\mathbf{S}\cdot\mathbf{I} + cS_{z'}I_{z'} - e\nabla\mathbf{E}\cdot\mathbf{Q}$, where $\hat{z}'$ is the molecular fixed internuclear axis, and the final term is the scalar product of two second-rank tensors representing the gradient of the electric field at the location of the bromine nucleus and the electric quadrupole moment of that nucleus. For $Ca^{79}Br$, the size of the spin-rotation and hyperfine terms are comparable: $\gamma_{sr} = 90.7$ MHz, $b = 95.3$ MHz, $c = 77.6$ MHz, and the electric quadrupole coupling constant $(eqQ)_0 = 20.0$ MHz (ref. 47).

CHIP-BASED MICROTRAPS FOR POLAR MOLECULES

In a polar molecule, the body-fixed electric dipole moment ($\boldsymbol{\mu}$) gives rise to large transition moments between rotational states, which are separated by energies corresponding to frequencies in the microwave range. The level structure of a diatomic rigid rotor is determined by the hamiltonian $H_{rot} = \hbar B\mathbf{N}^2$, where $\mathbf{N}$ is the rotational angular momentum, B is the rotational constant and $\hbar$ is the reduced Planck's constant. This hamiltonian gives energy levels $E_N = \hbar BN(N+1)$ that are $(2N+1)$-fold degenerate, corresponding to the different projections m_N. In the presence of a d.c. electric field $\boldsymbol{\mathcal{E}}_{d.c.}$, the Stark hamiltonian $H_{St} = -\boldsymbol{\mu}\cdot\boldsymbol{\mathcal{E}}_{d.c.}$ mixes rotational states and induces level shifts that break the degeneracy between states of different $|m_N|$. Two of the low-lying states, $|1\rangle \equiv |N=1\rangle \equiv |N=1, m_N=0\rangle$ and $|2\rangle \equiv |N=2\rangle \equiv |N=2, m_N=0\rangle$ with corresponding eigenenergies E_1 and E_2, are weak-field seeking; that is, their energy increases with larger $\mathcal{E}_{d.c.}$ (see Fig. 1). We take these two states as the working rotational qubit states for the system. As discussed below, qubits stored in spin or hyperfine states can be transferred to these rotational qubits with microwave pulses. A static electric field minimum can be formed in free space, allowing for trapping of these low-field-seeking molecules.

The maximum trap depth possible, determined by the maximum Stark shift of the $|1\rangle$ state, is $U_{max} \approx 0.6\hbar B$, attained at an electric field $\mathcal{E}_{d.c.}^{max} \sim 6\hbar B/\mu$. The energy splitting between rotational states, ω_0, is field dependent due to mixing with other $|N, m_N\rangle$ states. However, under all conditions discussed in this paper the relation $\omega_0 \equiv (E_2 - E_1)/\hbar = 4B$ is valid to within 10%. Explicit calculations of the molecular energy levels as a function of $\mathcal{E}_{d.c.}$ are shown in Fig. 1. For concreteness, throughout the paper we use CaBr in its ground vibrational state as our example molecule, although many others share the desired properties for quantum computation in our scheme. For CaBr, $\mu = 2\pi \times 2.25$ MHz V^{-1} cm (4.36 D), $B = 2\pi \times 2.83$ GHz, $U_{max} \approx 80$ mK, $\mathcal{E}_{d.c.}^{max} \approx 7 \times 10^3$ V cm^{-1} and $\omega_0 = 2\pi \times 11.3$ GHz.

A variety of macroscopic electrostatic traps for polar molecules have been proposed and/or implemented[13–15]. In the Methods section, we describe in detail a novel electrostatic 'EZ' trap (Fig. 2a). In brief, the EZ trap creates a non-zero electric field minimum in close proximity to the surface of a chip. With trap electrode dimensions ranging from $w = 0.1$ to 1 μm and corresponding voltages $V_{EZ} \sim 0.1$–1 V, $U_0 \sim U_{max}$ and $\omega_t \sim 2\pi \times 6$–0.6 MHz for CaBr.

To efficiently load the EZ trap, it is necessary to have a source of cold polar molecules that can achieve a phase-space density, Φ, comparable to that for a single molecule in the EZ trap, that is, $\Phi \sim w^{-3}U_0^{-3/2}$ ($\sim 10^{15}$ cm^{-3} K$^{-3/2}$ for our nominal conditions). Although this value is beyond that which has been achieved so far with polar molecules, it seems feasible with several methods currently under development. For example, cooled molecules (produced using, for example, techniques such as buffer-gas cooling[16] or Stark slowing[13]) could be trapped directly in the EZ trap or trapped in a larger, intermediate trap and then further cooled to increase Φ, using a variety of techniques. Possibilities, all still unproved with polar molecules, include evaporative[17–19] or sympathetic cooling, cavity cooling[20] or the stripline-assisted sideband cooling described below. With sufficient phase-space density, trap-door loading[13] and mode matching to a micrometre-sized EZ-trap configuration should be possible using electrostatic fields[21].

APPROACH TO CAVITY QED

Superconducting stripline resonators[22] can be used to confine microwave fields to an extremely small volume[23], $V \sim w^2\lambda \ll \lambda^3$, where λ is the resonant wavelength. One important consequence is the large vacuum Rabi frequency $g = \wp\mathcal{E}_0/\hbar$ for molecules

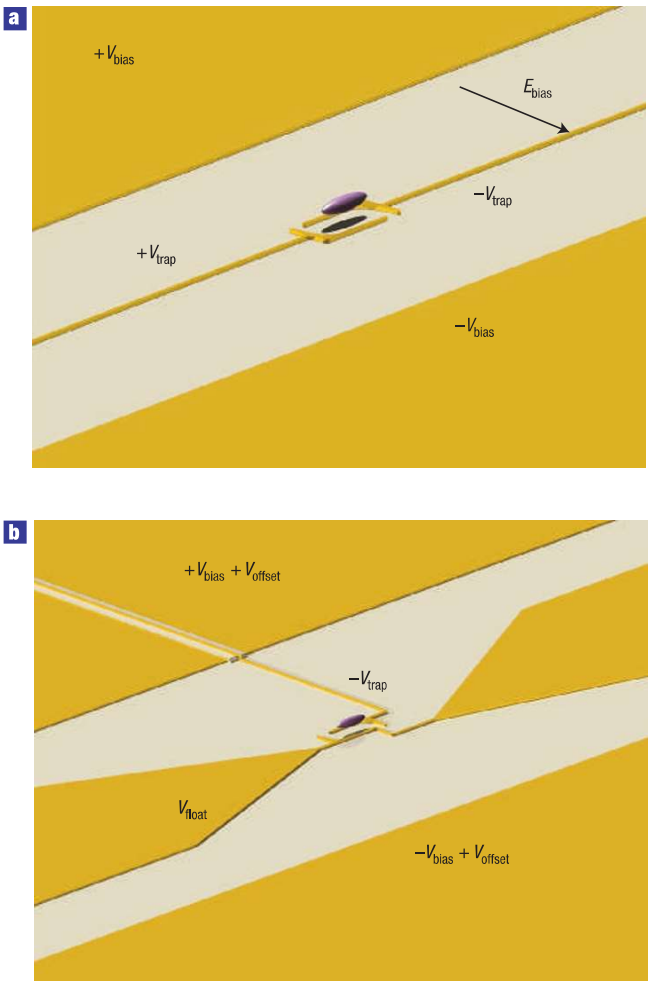

Figure 2 Electrostatic Z-trap. Schematic diagram of the proposed electric trap, the EZ trap, for holding polar molecules above a microwave stripline. **a**, EZ-trap design. The thin wire-like electrodes biased at $\pm V_{trap}$ generate the strong local electric field gradients needed for trapping. The trap is of the Ioffe–Pritchard type: there is no field zero, which avoids dipole flips from the field-aligned to the anti-aligned state (that is, a 'Majorana hole', which would allow coupling to the untrapped states with $m_N \neq 0$). **b**, Zoomed-out view of the EZ trap, integrated with a microwave stripline resonator. The ground planes of the resonator are biased at the d.c. voltages $\pm V_{bias} + V_{offset}$, giving rise to the bias field E_{bias} for the EZ trap. The offset voltage V_{offset} is used to bias the central pin and adjust V_{float}. In the region shown, which is of a much smaller size than the wavelength of the microwave photons carried by the stripline, the width of the central pin of the stripline resonator is gradually reduced and deformed to the shape of one of the L-shaped electrodes of the EZ trap. The second L-shaped electrode needed to form the EZ trap is made of a thin wire-like electrode overlaid on one of the conducting ground planes. This electrode can behave as a continuation of the ground plane for a.c. voltages at microwave frequencies, whereas at d.c. it can be independently biased at the voltage V_{trap}, thereby completing the EZ trap. The overall effect of the region where the central pin is thinner is a slight change in the capacitance per unit length, without significantly affecting the quality of the resonator.

located close to such a resonator, allowing coherent coupling of the molecule to the quantum state of the resonator field. (Here $\wp$ is the transition dipole matrix element and $\mathcal{E}_0 \propto V^{-1/2}$ is the zero-point electric field; $\wp \approx 0.5\mu$ under the relevant conditions.)

When the microwave field is confined to a resonator and is quantized, the coupling becomes the well-known[24] Jaynes–Cummings hamiltonian $\hat{H} = -\hbar g(\hat{a}^\dagger\hat{\sigma}^- + \hat{a}\hat{\sigma}^+)$, where $\hat{a}$ is the annihilation operator for the resonator mode, $\hat{\sigma}^- = |1\rangle\langle 2|$ is the lowering operator for the molecule, $\hat{\sigma}^+ = |1\rangle\langle 2|$ is the raising operator, and $|1\rangle, |2\rangle$ are the two states coupled by the field. The value of g can be calculated as follows (see also ref. 12). The stripline zero-point voltage is $V_0 = \sqrt{\hbar\omega/(2C)}$, where C is the effective capacitance of the stripline resonator. For impedance matching with standard microwave devices, $C = \pi/(2\omega Z_0)$, with $Z_0 = 50\,\Omega$. At a height z_0 above a stripline with conductor spacing w, the zero-point electric field is $\mathcal{E}_0 \sim f(z)V_0/w$. Here $f(z)$ is a dimensionless geometric factor describing the reduction of the field away from the electrodes; $f(z) = 1$ for $z \ll w$ and we find through simulation that $f(z) \sim 0.5(w/z)$ for $z \lesssim w$. For CaBr trapped at a height $z \lesssim w = 0.1$–$1\,\mu$m above the resonator, the single-photon Rabi frequency is in the range $g/2\pi \simeq 400$–$40\,$kHz.

High-Q resonators (internal Q values of 10^6 have been demonstrated[22,25,26]) lead to long microwave photon lifetime. When coupling to the resonator is stronger than the cavity decay rate ($\kappa = \omega/Q$), coherent quantum-state exchange between the polar molecule and the resonator field is possible. That is, for molecules held close to a small resonator, the electric dipole interaction with the resonator mode is strong enough to reach the strong coupling regime of cavity QED[27,28].

COOLING MECHANISM

Strong coupling of the molecule to the microwave cavity enhances spontaneous emission of excited rotational states, which can be used to cool the trapped molecules. When molecules are initially loaded into the trap, their temperature may be as high as the trap depth U_0, corresponding to a mean number of trap excitations $\bar{n}_t \sim U_0/(\hbar\omega_t)$, where ω_t is the trap frequency. Depending on the cold molecule production method used, $\bar{n}_t$ can be very large. As discussed below, the best coherence properties for molecular superposition states are achieved when the molecule is in the ground motional state of the trap. Hence, it is desirable to cool the motional degree of freedom. The tight confinement of the molecule in the EZ trap suggests sideband cooling, as done with trapped ions[29]. If the molecule was in free space this would not be possible due to the low natural decay rate of excited rotational states, $\gamma < 10^{-5}\,s^{-1}$. However, the cavity-enhanced spontaneous emission makes sideband cooling feasible (Fig. 3a). As described in the Methods section, a trapped molecule can be sideband cooled to the motional ground state of the trap with a rate much higher than the observed trap loss rates of atoms from microtraps—typically limited by background gas losses.

In the absence of any heating mechanisms, sideband cooling proceeds until the molecule's mean motional quantum number in the trap, $\bar{n}_t$, equals the mean number of thermal microwave photons in the resonator mode, $\bar{n}_\gamma$. Owing to the frequency mismatch between the resonator mode frequency ω and the trap frequency ω_t, the effective final temperature T_t of the trap degree of freedom is lower than the ambient resonator temperature, T_r, by the large factor $R = \omega_t/\omega$. For example, $T_t < 100\,\mu$K for $T_r = 100\,$mK. Technical noise sources may lead to a larger photon occupancy in the cavity than the nominal thermal value $\bar{n} = \exp(-\hbar\omega/kT_r) \sim 5 \times 10^{-3}$. However, it has been shown that $\bar{n}_\gamma \ll 1$ is achievable[22].

The location of the EZ trap centre is determined by the voltage on the electrodes (Fig. 2a), so that fluctuations of this voltage cause random motion of the trap centre and heating of the molecule's motion in the trap. As a worst case, we can assume that the micrometre-sized electrodes experience the typical $1/f$ charge noise, where f denotes frequency, as measured in work with single-electron transistors and charge qubits. These may be

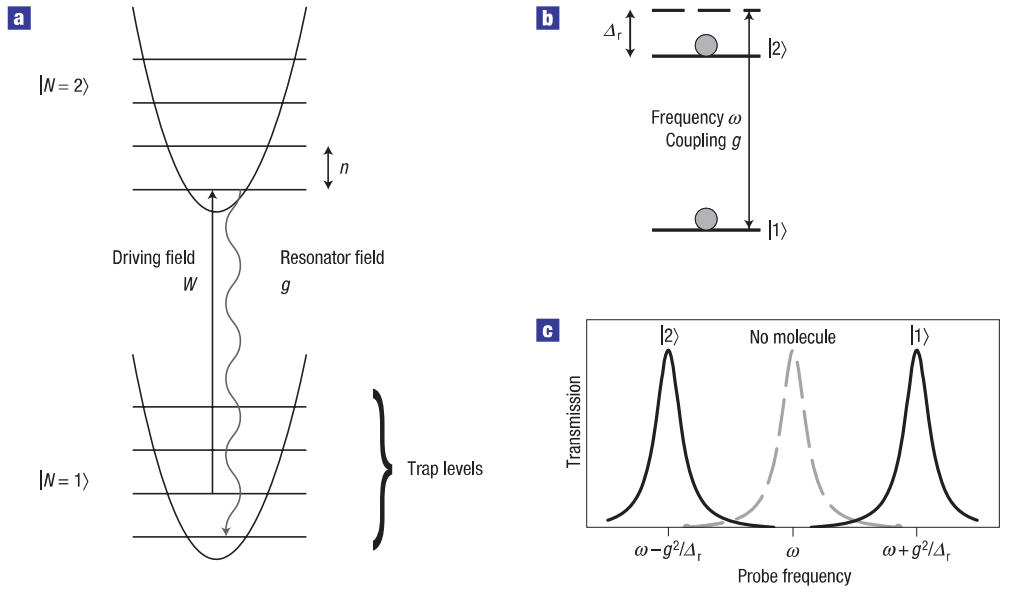

Figure 3 Resonator-enhanced sideband cooling and quantum state readout. a, Sideband cooling using resonator-enhanced spontaneous emission. The driving field is tuned to the red sideband $|1, n\rangle \rightarrow |2, n-1\rangle$, while the resonator is resonant with the $|2, n\rangle \rightarrow |1, n\rangle$ transition, where n denotes the trap motional level. **b**, Quantum-state readout via a dispersive shift of the cavity induced by the qubit. In the dispersive limit when the rotational transition of the molecule is significantly detuned from the cavity frequency ($\Delta_r \gg g$), a qubit-state-dependent frequency shift $\delta\omega = \pm g^2/\Delta_r$ allows non-demolition measurement of the molecule's state by probing the transmission or reflection from the cavity. In the limit $\delta\omega < \kappa$, microwaves transmitted at the cavity frequency undergo a phase shift of $\pm\tan^{-1}(2g^2/\kappa\Delta_r)$ when the qubit is in state $|1\rangle, |2\rangle$ respectively. For readout, the cavity-qubit detuning is set to $\Delta = \Delta_r$ (see the Methods section). **c**, Probe field transmission versus probe frequency. When $g^2/\Delta_r > \kappa$, the frequency shift of the cavity is larger than the resonator linewidth. A probe beam at one or the other of the new, shifted frequencies will be transmitted or reflected, again allowing a potentially high-fidelity readout of the qubit state. In the absence of molecules, no frequency shift occurs, so the presence or absence of molecules in the trap can also be determined.

roughly analogous (at micrometre size and mK temperatures) to the 'patch potentials' observed in ion traps[30]. The typical charge noise[31] density S_Q has a $1/f$ dependence, with magnitude $S_Q(f) = 10^{-6}$–$10^{-7}e^2/f$; on a metal electrode with $C_t \sim 1$ fF (typical for micrometre-scale features), the corresponding voltage spectral density is $S_V(f) = S_Q/C_t^2 \sim (10^{-14}/f)\ \mathrm{V^2\,Hz^{-1}}$. With the trap operating in the linear Stark regime, the heating rate, defined as the rate of excitation from $|0\rangle$ to $|1\rangle$, is $\Gamma_{01} \sim \omega_t^2(w/a_0)^2(S_V(\omega_t)/V_{EZ}^2)$ Hz, where $a_0 = \sqrt{\hbar/(2m\omega_t)}$ is the ground-state wavefunction width, and V_{EZ} is the voltage on the trap electrodes as described in the Methods section. Under our conditions $\Gamma_{01} \ll 2\pi \times 1$ Hz (ref. 32), indicating that cooling to $\bar{n} \ll 1$ should be feasible. The rate of heating in a real device, along with the actual dephasing rates for a molecule near the surface of a chip, are important phenomena which must be experimentally determined.

POLAR MOLECULES AS QUANTUM BITS

Trapped polar molecules, cooled close to their ground state of motion in the EZ trap and coupled to stripline resonators, represent a good starting point for quantum bits. For quantum processing, the qubit can be encoded in a pair of trapped rotational states ($|1\rangle$ and $|2\rangle$) and single-qubit operations carried out using classical microwave fields. Molecules coupled through stripline resonators allow for two-qubit operations. The detuning of each molecule from the resonator, Δ, can be adjusted locally by changing the trap bias field $\mathcal{E}_{d.c.}^{off}$ as required for various types of operations (as described below).

We now consider coherence properties of rotational superpositions. The resonator-enhanced spontaneous emission rate is $\Gamma_{21} = \kappa g^2/\Delta^2$, which can be suppressed to a negligible level ($\Gamma_{21} < 2\pi \times 1$ Hz) by keeping Δ sufficiently large ($\Delta > 2\pi \times 10$ MHz under our nominal conditions). Voltage fluctuations in the trap electrodes (quantified by $S_V(f)$) are more troublesome, they cause random fluctuations of the qubit transition frequency, and hence dephasing of rotational superposition states. Decoherence due to this voltage noise is determined by the field sensitivity of the rotational splitting, $\partial\omega_0/\partial\mathcal{E}$, and the effective r.m.s. variations of the trap voltage, $V_{r.m.s.}^{eff}$. Properly accounting for qubit phase fluctuations from a $1/f$ spectrum[33], $V_{r.m.s.}^{eff} \sim 0.2\,\mu$V. In the linear Stark regime, and over a wide range of electric fields, the electric field sensitivity of the qubit transition frequency is $|\partial\omega_0/\partial\mathcal{E}| \approx 0.1\mu/\hbar \approx 2\pi \times 200\,\mathrm{kHz\,(V\,cm^{-1})^{-1}}$ for CaBr, leading to r.m.s. frequency shifts $\delta\omega_0 = (\partial\omega_0/\partial\mathcal{E})V_{r.m.s.}^{eff}/w$. For short times, this results in quadratic decay of qubit coherence[34], with a characteristic rate $\gamma_V \sim \delta\omega_0 = 2\pi \times 4$–$0.4$ kHz.

Although the trap potential is, in general, different for the two rotational qubit states, as assumed above, there is a specific offset field value—a 'sweet spot'—for which the trap curvature is the same. (This occurs at $\mathcal{E}_{d.c.}^{off,sweet} \approx 3\hbar B/\mu$.) When the trap is biased at this sweet spot, $|\partial\omega_0/\partial\mathcal{E}| = 0$ for the lowest vibrational levels of the trap. The second-order term is given by $\left|\partial^2\omega_0/\partial\mathcal{E}^2\right| \approx 0.1\mu^2/(\hbar^2 B)$. In CaBr this is given numerically by $\delta\omega_0/\mathcal{E}_{d.c.}^2 = 2\pi \times 100\,\mathrm{Hz\,(V\,cm^{-1})^{-2}}$. Decoherence due to voltage noise can thus be vastly reduced by operating at the sweet spot, where $\delta\omega_0 \approx \left|\partial^2\omega_0/\partial\mathcal{E}^2\right|(V_{r.m.s.}^{eff}/w)^2$ and $\gamma_{V,2} \sim \delta\omega_0$ is below the 1 Hz level. Operation at the sweet spot comes with the modest expense of reducing the maximum possible trap depth by a factor of four.

Molecular motion also causes variations in the qubit level splitting, and thus also dephases rotational qubits. If the molecule

is in its motional ground state, $\bar{n} = 0$, it can be kept there during microwave manipulation of the qubit (provided the excitation rate is slower than the trap frequency). In the case of finite molecular temperature, the rotational superpositions will dephase with a characteristic rate $\gamma_T \sim (\omega_t^2/B)\bar{n}^2$. If $\bar{n} \sim 1$ and $\omega_t \sim 2\pi \times 5$ MHz, then $\gamma_T \sim 2\pi \times 1$ kHz. Thus, cooling of the molecular motion is crucial for long-lived rotational coherences.

Single-qubit quantum gates can be accomplished by driving rotational transitions with oscillating electric fields. During such a gate operation (driven at Rabi frequency Ω), the error probability p is bounded by $p \leq (\gamma^*/\Omega)^2$ per single Rabi cycle, where $\gamma^* \equiv \gamma_T + \gamma_{V,2}$ is a total dephasing rate for rotationally encoded qubits. Taking, for example, $\Omega \sim 2\pi \times 1$ MHz (consistent with all constraints on the system), we find that p is negligible for our operating conditions.

Finally, we note that for quantum storage the qubits can also be encoded in hyperfine 'clock' ($m = 0$) or Zeeman spin sublevels of a single rotational state, in which low dephasing can be obtained even away from the sweet spot. As discussed below, such encoding might facilitate scalability of the polar-molecule quantum computer. Our example case of CaBr has one nuclear spin $I = 3/2$ and one unpaired electron spin, with a molecular state $^2\Sigma^+$. Figure 1a shows the energy levels of selected states in an electric field. Within a broad range of electric field values, the value of $|\partial\omega/\partial\mathcal{E}|$ for transitions between hyperfine sublevels with magnetic quantum number $M_{F_3} = 0$ is $\sim 10^3$ smaller than for rotational transitions away from the sweet spot. Zeeman sublevels whose splittings are completely insensitive to electric fields also exist (although these introduce new features beyond the scope of this paper). Note that hyperfine level degeneracies do not impose additional restrictions on one-bit gate speeds; for CaBr near the sweet spot, the rotational transitions differ by $\delta\omega_h \approx 15$ MHz for two hyperfine states.

LONG-RANGE QUANTUM COUPLING

We conceive a two-qubit gate protocol as follows. In a resting state (no gate operations being carried out), qubits will be encoded in hyperfine sublevels of the $|1\rangle$ state. To carry out a two-bit gate protocol, the two selected bits will be activated by writing the information into the rotational superposition state, via microwave pulses tuned to resonance by adjustment of the trap bias fields of the selected bits. Once activated, the two selected qubits can be made to interact by tuning both to a common value of Δ. The ease of control by microwave and quasi-static electric fields coupled entirely by wires on a chip, and the ability to have highly selective addressability of molecules due to the relatively large separation (mm) between trap sites, make this proposed scheme attractive for scaling.

We now consider in detail coherent interactions of polar molecules through the capacitive, electrodynamic coupling to superconducting transmission line resonators[12,23]. For simplicity, we consider a so-called $\sqrt{\text{SWAP}}$ operation[2] between a pair of rotational qubits. As illustrated in Fig. 4, we use an off-resonant interaction with detuning Δ between the resonator and qubit, with the molecules located at voltage nodes along the resonator. Assuming $\Delta \gg g$ and adiabatically eliminating the resonator degree of freedom, we find an interaction of the form $H_{\text{int}} = (g^2/\Delta)\left(\hat{\sigma}_1^+\hat{\sigma}_2^- + \hat{\sigma}_1^-\hat{\sigma}_2^+\right)$, where g^2/Δ is the interaction rate and $\hat{\sigma}_i^- = |1\rangle\langle 2|_i$ is the lowering operator for the ith molecule. This effective exchange interaction can be used to map coherent superpositions from one quantum bit to another in time $\tau = \pi\Delta/2g^2$, thus allowing a universal two-qubit gate[35]. Note that at large molecule-resonator detuning ($\Delta \gg \kappa$), the resonator mode is only virtually occupied, so that cavity decay has little effect: the probability of error due to spontaneous emission of a photon during the two-bit gate is $p_{\text{sp}} = \kappa g^2/\Delta^2\tau = (\pi/2)(\kappa/\Delta)$.

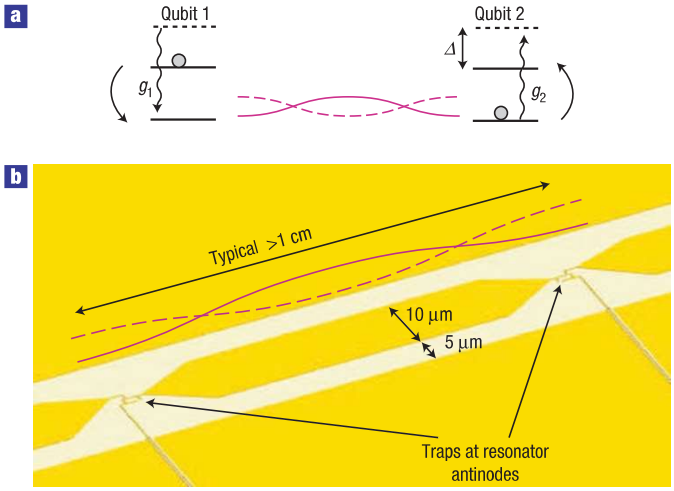

Figure 4 Capacitive coupling of molecules mediated by a stripline. **a**, Polar-molecule qubits are coupled to each other via (off-resonant) virtual exchange of microwave photons through a stripline resonator. The detuning between the resonator mode and the qubit frequency is Δ, and the qubits are coupled to the resonator mode with the same vacuum Rabi frequencies g. The effective dipole–dipole interaction mediated by the resonator is given by the hamiltonian $H_{\text{int}} = (g^2/\Delta)\left(\hat{\sigma}_1^+\hat{\sigma}_2^- + \hat{\sigma}_1^-\hat{\sigma}_2^+\right)$. As indicated schematically in the figure, this interaction corresponds to qubit 1 emitting a virtual photon in the resonator while changing state from the upper to the lower state, and qubit 2 absorbing the virtual photon while changing state from the lower to the upper state. **b**, Multiple EZ traps can be patterned along the length of a stripline resonator, allowing coupling of multiple qubits. Here two EZ traps located at the resonator mode antinodes are shown, with typical dimensions indicated.

Slower gate speed (at large detuning Δ) results in reduced p_{sp}, and also in increased probability of dephasing $p_{\text{dep}} = (\gamma^*\tau)^2$. The overall probability of error $p_{\text{err}} = p_{\text{sp}} + p_{\text{dep}}$ is minimized by choosing $\Delta^* = \left(g^4\kappa/\pi\gamma^{*2}\right)^{1/3}$, resulting in a total error probability $p_{\text{err}} \approx (\kappa\gamma^*/g^2)^{2/3}$. For example, with $\kappa = 2\pi \times 10$ kHz ($Q = 10^6$), $g = 2\pi \times 200$ kHz and $\gamma^* \sim 2\pi \times 1$ kHz, we find that at the optimal detuning the probability of error is well below 1%. Thus, high-fidelity two-qubit operations between remote qubits are possible.

STATE-DEPENDENT DETECTION

The presence of a trapped molecule, as well as its internal state, can be detected by measuring the phase shift of an off-resonant microwave field transmitted through the resonator (Fig. 3b). The dispersive interaction of the dipole and resonator leads to a state-dependent phase shift of the resonator field[22], implementing a near-perfect quantum non-demolition measurement of the qubit state. This method has already been used to detect superconducting qubits[3], and it can also be applied to detect the quantum state of molecules with high signal-to-noise ratio. As shown in the Methods section, very high-fidelity (>99%) readout of the polar-molecule qubit is feasible.

POTENTIAL FOR SCALING QUANTUM CIRCUITS

To realize scalable quantum information processors, or to implement quantum error correction on logical qubits and high-fidelity quantum gates, the physical qubits need to be connected to each other through quantum channels. In addition, quantum

information needs to be moved around the network efficiently. To implement a logical qubit suitable for error correction, the proximity of several physical qubits is required, any pair of which can be subjected to a quantum gate. A possible solution involves an array of storage zones where molecules are trapped, cooled and initialized via their coupling to stripline resonators. Furthermore, in analogy to ion trap approaches[36], qubits stored in hyperfine or Zeeman sublevels of a single rotational state may be moved to interaction zones using electrostatic gates. Moving and coupling of qubits could be achieved by patterning multiple EZ traps in the gap between the two ground planes of a stripline resonator.

In this scheme, we conceive qubit transport in hyperfine/Zeeman states to relevant interaction zones and processing in rotational states. When a particular qubit is needed to carry out a quantum operation, it can be transferred from storage to a rotational state using frequency-selective microwave transitions. Taking the example of CaBr encoded in hyperfine states, dephasing from either voltage noise or finite temperature of the molecule is suppressed during storage and transport to very low levels. Specifically, over a broad range of electric field values, a hyperfine qubit associated with a motionally excited molecule will dephase at a rate scaling as $\gamma_{\mathrm{T}}^{\mathrm{hf}} \sim \omega_{\mathrm{t}}\bar{n}/10^3$. This implies that for reasonably cold molecules, $\bar{n} = 1$, trap potentials can be changed adiabatically (that is, with negligible motional heating) on a timescale much faster than for qubit dephasing. The hyperfine qubit can be transferred to rotational states when the molecule is brought back to the sweet spot. Finally, we note that it may be possible to cool the molecule's motion without destroying hyperfine/Zeeman state coherence, provided that the detuning between the cavity and qubit is much larger than hyperfine/Zeeman level splitting. Thus, potentially scalable quantum circuits could be designed using polar molecules as quantum bits and superconducting resonators as the quantum bus connecting these qubits. We emphasize that the present approach combines the key elements required for building a scalable quantum processor, including the potential for the creation and intialization of multiple qubits, long-term quantum memory, high-fidelity quantum gates, the ability to carry out parallel operations, and exceptional qubit connectivity. By analogy with detailed analysis carried out for ion trap approaches[37], favourable thresholds for fault-tolerant operation can be expected for our approach.

OUTLOOK

A number of other interesting avenues can be considered. For example, the excellent coherence properties of hyperfine states of polar molecules may provide a long-term quantum memory for solid-state qubits. Specifically, coupling to a stripline resonator can be used to map the quantum state of a superconducting qubit[3–5] to the state of a single molecule. Moreover, in this case coupling strength can be enhanced by using a collective excitation of a small molecular ensemble, as described in ref. 38. These approaches can be further used to provide an interface to 'flying' qubits. Molecular microwave-frequency qubits can be mapped via a Raman process to single photons in the infrared or optical regime (corresponding to vibrational and electronic molecular transitions, respectively)[39]. In addition, novel approaches to controlled many-body physics can be predicted. Tightly confined polar molecules in high-aspect-ratio EZ traps can be used to realize a one-dimensional quantum system with strong, long-range interactions. Coupling to the stripline may provide a novel tool for preparation of such strongly interacting systems, as well as for detecting the resulting quantum phases[40]. Finally, we also note other work on this possibility including the use of molecular vibrational states[41–43]. Such possibilities could be combined with the ideas outlined here.

We emphasize that the approach described here is unique in that it combines tight localization, fast manipulation and electrical gate control, unprecedented for single-particle systems, with exceptional coherence properties which are uncommon for condensed-matter approaches. Although the techniques for production of cold polar molecules are not developed as well as those for charged ions and neutral atoms, exciting recent experimental progress indicates that the ideas proposed here are within experimental reach.

METHODS

SIDEBAND COOLING THROUGH ENHANCED SPONTANEOUS EMISSION

The absorption spectrum of the trapped molecule in the combined rotational ($N = 1, 2$) and motional (n) states, $|N, n\rangle$, consists of a carrier at frequency ω_0 and sidebands at frequencies $\omega_0 + (m-n)\omega_{\mathrm{t}}$ ($n, m = 0, 1, \ldots$). Electromagnetic coupling to sidebands arises due to the position dependence of g. Sideband cooling occurs when a driving field is tuned to the lower-energy sideband $|1, n\rangle \rightarrow |2, n-1\rangle$, while the resonator mode is resonant with the $|2, n\rangle \rightarrow |1, n\rangle$ transition (Fig. 3a). Each scattering cycle reduces the kinetic energy of the molecule by $\hbar\omega_{\mathrm{t}}$. If $\kappa < \omega_{\mathrm{t}}$, the sidebands can be resolved. The lower-energy sideband state can either be directly excited by an on-resonant driving field or virtually excited by a red-detuned field. De-excitation occurs by emitting a photon into the resonator, which can then decay out of the resonator. The maximum cooling rate can be estimated as follows. For $g \ll \kappa$ ($g \gtrsim \kappa$), the cavity-enhanced spontaneous emission rate for the cavity tuned to resonance, $\omega = \omega_0$, is given by $\Gamma_{\mathrm{c}} = g^2/\kappa$ ($\Gamma_{\mathrm{c}} = \kappa/2$). For example, with $g = 2\pi \times 40$–400 kHz and $\kappa = 2\pi \times 10$ kHz ($Q = 10^6$), $\Gamma_{\mathrm{c}} \sim 2\pi \times 5$ kHz; this yields a cooling rate $\mathrm{d}n/\mathrm{d}t = \Gamma_{\mathrm{c}}$ and hence $\mathrm{d}E/\mathrm{d}t = \hbar\omega_{\mathrm{t}}\Gamma_{\mathrm{c}} \approx 10\,\mathrm{K\,s^{-1}}$ for trapping frequency $\omega_{\mathrm{t}} \sim 2\pi \times 5$ MHz. A detailed analysis follows.

We assume the molecule is in a harmonic trap of frequency ω_{t}, a distance z above a stripline resonator of resonant frequency ω, as shown in Fig. 3a. The resonator is tuned close to the resonance frequency ω_0 of the molecular dipole transition $|1\rangle \rightarrow |2\rangle$. The height of the molecule above the resonator can be written as $z = z_0 + \hat{z}$, where $\hat{z}$ is the displacement from the equilibrium position in the trap. We write $\hat{z} = a_0\hat{x}$. Then $\hat{x} = (\hat{b} + \hat{b}^{\dagger})$ is a dimensionless position operator, with $\hat{p} = -i(\hat{b} - \hat{b}^{\dagger})$ its conjugate momentum, so that in the ground state $\Delta x = \Delta p = 1$. Introducing the effective Lamb–Dicke parameter $\eta = a_0/z_0 \ll 1$ in analogy with sideband cooling in ion traps[29], we have $g(\hat{x}) = g_0\left[1 - \eta\hat{x} + \mathrm{O}[\eta^2]\right]$. For our nominal parameters we find $a_0 \simeq 3$ nm, so that for CaBr trapped at $z_0 = 100$ nm, $\eta \simeq 0.03$.

For cooling, the resonator is pumped by an external field tuned to the red sideband, while the resonator field is resonant with the dipole transition, as shown in Fig. 3a. The coupling of the resonator field to the molecular dipole is described by the interaction hamiltonian

$$\hat{H} = \omega_{\mathrm{t}} b^{+} b^{-} + g_0(\hat{a}^{\dagger}\sigma_{-} + \sigma_{+}\hat{a}) + \eta g_0 \hat{x}(\hat{a}^{\dagger}\sigma_{-} + \sigma_{+}\hat{a}).$$

A general analysis based on perturbation theory using the small parameter η can be used to obtain the cooling rates[44]. We can also obtain approximate analytic expressions for the cooling rates in a simple regime of sideband cooling when $\omega_{\mathrm{t}} \gg \kappa \gg g_0$. In this case the cavity field can be adiabatically eliminated, resulting in effective spontaneous decay of the excited rotational state at rate $\gamma_{\mathrm{sp}} = 2g^2/\kappa$. The sideband excitation rate R from a coherent microwave drive with Rabi frequency Ω is given by $R = \eta^2\Omega^2/\gamma_{\mathrm{sp}}$. The cooling rate is then given by $\Gamma_{\mathrm{c}} = \gamma_{\mathrm{sp}}R/(2R + \gamma_{\mathrm{sp}}) \rightarrow \gamma_{\mathrm{sp}}/2$ in the limit of strong driving. This rate is ultimately limited by cavity decay $\kappa/2$ when the strong coupling regime is reached.

The resonator and trap degree of freedom exchange quanta until they equilibrate to the same mean number of quanta, which is set by the background (for example, thermal) number of photons in the microwave cavity. Note that although we only describe cooling of the degree of freedom perpendicular to the chip surface, similar considerations can be applied to all trap degrees of freedom. Finally, we note that the trapping potentials experienced by the molecule in the upper and lower states may be different, and that the trap potentials are significantly anharmonic before cooling near the ground state. However, sideband cooling can still occur in this regime and leads to similar cooling rates and final temperatures as described above.

THE EZ TRAP AND THE EFFECT OF THE SURFACE ON TRAPPED MOLECULES

A variety of macroscopic electrostatic traps for polar molecules have been proposed and/or implemented[13–15]. Here, we describe a novel EZ trap (Fig. 2a), a mesoscopic electric trap that is closely related to the magnetic Z trap[6], which is widely used in miniature atomic traps. The EZ trap creates a non-zero electric field minimum in close proximity to the surface of a chip. The field at the bottom of the trap is designated $\mathcal{E}_{\mathrm{d.c.}}^{\mathrm{off}}$. Metallic electrodes set to the appropriate d.c. voltages give rise to the inhomogeneous trapping field. Adjustment of the trap and bias electrodes sets the trap depth as well as $\mathcal{E}_{\mathrm{d.c.}}^{\mathrm{off}}$ and the position of the trap centre, typically at height $z_0 \sim w$ above the surface, where w is the spacing between the trap electrodes.

With EZ trap electrodes that are thin compared with w and held at voltage V_{EZ}, maximum d.c. electric fields $\mathcal{E}_{\mathrm{d.c.}}^{\mathrm{max}} \sim V_{\mathrm{EZ}}/w$ can be generated, leading to harmonic trap potentials with depth $U_0 \sim 0.1\mu\mathcal{E}_{\mathrm{d.c.}}^{\mathrm{max}}$ and motional frequency $\omega_{\mathrm{t}} \sim \sqrt{2U_0/(mw^2)}$ for a molecule of mass m. With electrode dimensions ranging from $w = 0.1$ to 1 μm and corresponding voltages $V_{\mathrm{EZ}} \sim 0.1$–1 V, $U_0 \sim U_{\mathrm{max}}$ and $\omega_{\mathrm{t}} \sim 2\pi \times 6 - 0.6$ MHz for CaBr.

For a molecule at a small distance z above a conducting surface ($z < \omega/c$, where ω is the frequency of the dominant transition contributing to the dipole moment), there is a van der Waals potential due to the attraction of the molecule to its image dipole[45]. The potential is given approximately by

$$U(z) = \frac{\mu^2}{4\pi\epsilon_0(2z)^3} = \frac{C_3}{z^3} \approx \frac{20\ (\mu\mathrm{m}^3)}{z^3}\ \mathrm{nK},$$

for CaBr, where ϵ_0 is the permittivity of free space. Note that retardation does not modify the potential on the micrometre scale, in contrast to the case of atoms, because of the long wavelength of the transition which contributes most to the dipole moment. In addition, the trap frequency is modified by the z^{-3} potential and becomes $\omega_{\mathrm{t}}' = \sqrt{\omega_{\mathrm{t}}^2 - (12C_3/mz^5)}$ for a harmonic potential centred at z_0. At $z_0 = 100$ nm and $\omega_{\mathrm{t}} = 2\pi \times 6$ MHz, the change in the trapping frequency $\Delta\omega_{\mathrm{t}}/\omega_{\mathrm{t}} \ll 1\%$ and there is no effect on the trap depth due to the van der Waals interaction. The trap depth begins to be affected for the case of smaller z_0 or weaker confinement. For example, for $z_0 = 100$ nm and $\omega_{\mathrm{t}} = 2\pi \times 1$ MHz, the van der Waals potential shifts the trapping frequency by 2% and reduces the maximum trap depth from ~3 mK (set by the surface at $z = 0$) to <1 mK.

STATE-DEPENDENT DETECTION

Here, we consider an example of state-dependent detection of a single molecule using dispersive phase shift. Consider a stripline with $Q = 10^6$, a trap width of 0.5 μm giving a vacuum Rabi frequency of $g = 2\pi \times 125$ kHz and a detuning of $\Delta_{\mathrm{r}} = 2\pi \times 14$ MHz. In this case, the phase shift of a microwave probe beam is $\theta_0 = \tan^{-1}[2g^2/\kappa\Delta_{\mathrm{r}}] \sim 10°$. To remain in the dispersive limit[23], this phase shift can be measured using a probe beam with up to $n_{\mathrm{crit}} = \Delta_{\mathrm{r}}^2/4g^2 \sim 1{,}000$ photons, or an incident power $P_{\mathrm{read}} = n_{\mathrm{crit}}\hbar\omega_{\mathrm{r}}\kappa \sim 10^{-15}$ W. The signal-to-noise ratio in one cavity lifetime is given by $\mathrm{SNR} = \sin^2[\theta_0](n_{\mathrm{crit}}/n_{\mathrm{amp}}) \sim 6$, where $n_{\mathrm{amp}} = k_{\mathrm{B}}T_N/\hbar\omega_{\mathrm{r}} \sim 20$ is the noise added by a cryogenic amplifier with a noise temperature of $T_N \sim 5$ K. During the readout, the rotational state of the molecule can still decay by spontaneous emission via the cavity at a rate $\gamma_\kappa = \kappa(g^2/\Delta_{\mathrm{r}}^2)$, leading to a lifetime $T_1 = 1/\gamma_\kappa \sim 200$ ms; here the maximum signal-to-noise ratio of the measurement is improved by a factor $\kappa/\gamma_\kappa \sim 10{,}000$, showing that very high-fidelity (>99%) readout is feasible.

Received 2 May 2006; accepted 27 July 2006; published 27 August 2006.

References

1. Special issue on ultracold polar molecules: Formation and collisions *Eur. Phys. J. D* **31,** 149–444 (2004).
2. Loss, D. & DiVincenzo, D.P. Quantum computation with quantum dots. *Phys. Rev. A* **57,** 120–126 (1998).
3. Wallraff, A. *et al.* Approaching unit visibility for control of a superconducting qubit with dispersive readout. *Phys. Rev. Lett.* **95,** 060501 (2005).
4. Makhlin, Y., Schön, G. & Shnirmam, A. Quantum-state engineering with Josephson-junction devices. *Rev. Mod. Phys.* **73,** 357–400 (2001).
5. Nakamura, Y., Pashkin, Y. & Tsai, J. Coherent control of macroscopic quantum states in a single-cooper-pair box. *Nature* **398,** 786–788 (1999).
6. Folman, R., Krüger, P., Schmiedmayer, J., Denschlag, J. & Henkel, C. Microscopic atom optics: From wires to an atom chip. *Adv. At. Mol. Opt. Phys.* **48,** 263–273 (2002).
7. Mandel, O. *et al.* Controlled collisions for multi-particle entanglement of optically trapped atoms. *Nature* **425,** 937–940 (2003).
8. Cirac, J. I. & Zoller, P. New frontiers in quantum information with atoms and ions. *Phys. Today* **57,** 38–39 (2004).
9. Leibfried, D. *et al.* Creation of a six-atom 'Schrodinger cat' state. *Nature* **438,** 639–642 (2005).
10. Häffner, H. *et al.* Scalable multiparticle entanglement of trapped ions. *Nature* **438,** 643–646 (2005).
11. DeMille, D. Quantum computation with trapped polar molecules. *Phys. Rev. Lett.* **88,** 067901 (2002).
12. Sørensen, A. S., van der Wal, C. H., Childress, L. I. & Lukin, M. D. Capacitive coupling of atomic systems to mesoscopic conductors. *Phys. Rev. Lett.* **92,** 063601 (2004).
13. Bethlem, H. L. *et al.* Electrostatic trapping of ammonia molecules. *Nature* **406,** 491–494 (2000).
14. Rieger, T., Junglen, T., Rangwala, S. A., Pinkse, P. W. H. & Rempe, G. Continuous loading of an electrostatic trap for polar molecules. *Phys. Rev. Lett.* **95,** 173002 (2005).
15. Xia, Y., Deng, L. & Yin, J. Electrostatic guiding of cold polar molecules on a chip. *Appl. Phys. B* **81,** 459–464 (2005).
16. Egorov, D., Lahaye, T., Schöllkopf, W., Friedrich, B. & Doyle, J. M. Buffer-gas cooling of atomic and molecular beams. *Phys. Rev. A* **66,** 043401 (2002).
17. Weinstein, J. D., deCarvalho, R., Hancox, C. I. & Doyle, J. M. Evaporative cooling of atomic chromium. *Phys. Rev. A* **65,** 021604 (2002).
18. DeMille, D., Glenn, D. & Petricka, J. Microwave traps for cold polar molecules. *Eur. Phys. J. D* **31,** 375–384 (2004).
19. Masuhara, N. *et al.* Evaporative cooling of spin-polarized atomic hydrogen. *Phys. Rev. Lett.* **61,** 935–938 (1988).
20. Vuletic, V., Chan, H. W. & Black, A. T. Three-dimensional cavity Doppler cooling and cavity sideband cooling by coherent scattering. *Phys. Rev. A* **64,** 033405 (2001).
21. Bochinski, J., Hudson, E. R., Lewandowski, H., Meijer, G. & Ye, J. Phase space manipulation of cold free radical OH molecules. *Phys. Rev. Lett.* **91,** 243001 (2003).
22. Wallraff, A. *et al.* Strong coupling of a single photon to a superconducting qubit using circuit quantum electrodynamics. *Nature* **431,** 162–167 (2004).
23. Blais, A., Huang, R.-S., Wallraff, A., Girvin, S. M. & Schoelkopf, R. J. Cavity quantum electrodynamics for superconducting electrical circuits: An architecture for quantum computation. *Phys. Rev. A* **69,** 062320 (2004).
24. Scully, M. & Zubairy, M. S. *Quantum Optics* (Cambridge Univ. Press, Cambridge, 1997).
25. Day, P. K. *et al.* A broadband superconducting detector suitable for use in large arrays. *Nature* **425,** 817–821 (2003).
26. Frunzio, L., Wallraff, A., Schuster, D., Majer, J. & Schoelkopf, R. Fabrication and characterization of superconducting circuit QED devices for quantum computation. *IEEE Trans. Appl. Supercond.* **15,** 860–863 (2005).
27. Raimond, J. M. *et al.* Probing a quantum field in a photon box. *J. Phys. B* **38,** S535–S550 (2005).
28. Miller, R. *et al.* Trapped atoms in cavity QED: Coupling quantized light and matter. *J. Phys. B* **38,** S551–S565 (2005).
29. Wineland, D. J. & Itano, W. M. Laser cooling of atoms. *Phys. Rev. A* **20,** 1521–1540 (1979).
30. Deslauriers, L. *et al.* Zero-point cooling and low heating of trapped $^{111}Cd^+$ ions. *Phys. Rev. A* **70,** 043408 (2004).
31. Zorin, A. *et al.* Background charge noise in metallic single-electron tunneling devices. *Phys. Rev. B* **53,** 13682–13687 (1996).
32. Turchette, Q. A. *et al.* Heating of trapped ions from the quantum ground state. *Phys. Rev. A* **61,** 063418 (2000).
33. Astafiev, O., Pashkin, Y. A., Nakamura, Y., Yamamoto, T. & Tsai, J. Quantum noise in the Josephson charge qubit. *Phys. Rev. Lett.* **93,** 267007 (2004).
34. Schriefl, J., Makhlin, Y., Shnirman, A. & Schoen, G. Decoherence from ensembles of two-level fluctuators. *New J. Phys.* **8,** 001 (2006).
35. Cirac, J. I. & Zoller, P. Quantum computation with cold trapped ions. *Phys. Rev. Lett.* **74,** 4091–4094 (1995).
36. Kielpinski, D., Monroe, C. & Wineland, D. J. Architecture for a large-scale ion-trap quantum computer. *Nature* **417,** 709–711 (2002).
37. Steane, A. Overhead and noise threshold of fault-tolerant quantum error correction. *Phys. Rev. A* **68,** 042322 (2003).
38. Rabl, P. *et al.* Hybrid quantum processors: molecular ensembles as quantum memory for solid state circuits. *Phys. Rev. Lett.* **97,** 033003 (2006).
39. Lukin, M. D. Colloquium: Trapping and manipulating photon states in atomic ensembles. *Rev. Mod. Phys.* **75,** 457–472 (2003).
40. Sachdev, S. *Quantum Phase Transitions* (Cambridge Univ. Press, New York, 1999).
41. Troppmann, U., Tesch, C. M. & de Vivie-Riedle, R. Preparation and addressability of molecular vibrational qubit states in the presence of anharmonic resonance. *Chem. Phys. Lett.* **378,** 273–280 (2003).
42. Babikov, D. Accuracy of gates in a quantum computer based on vibrational eigenstates. *J. Chem. Phys.* **121,** 7577–7585 (2004).
43. Yelin, S. F., Kirby, K. & Côté, R. Schemes for robust quantum computation with polar molecules. Preprint at <http://xxx.lanl.gov/abs/quant-ph/0602030> (2006).
44. Cirac, J. I., Blatt, R., Zoller, P. & Phillips, W. D. Laser cooling of trapped ions in a standing wave. *Phys. Rev. A* **46,** 2668–2681 (1992).
45. Lin, Y., Teper, I., Chin, C. & Vuletic, V. Impact of the Casimir-Polder potential and Johnson noise on Bose-Einstein condensate stability near surfaces. *Phys. Rev. Lett.* **92,** 050404 (2004).
46. Brown, J. M. & Carrington, A. *Rotational Spectroscopy of Diatomic Molecules* (Cambridge Univ. Press, New York, 2003).
47. Childs, W. J., Cok, D. R., Goodman, G. L. & Goodman, L. S. Hyperfine and spinrotational structure of CaBr $X\,^2\Sigma(v = 0)$ by molecular-beam laser-rf double resonance. *J. Chem. Phys.* **75,** 501–507 (1981).

Acknowledgements

We thank T. Calarco, L. Childress, A. Sorensen and J. Taylor for helpful discussions. Work at Harvard is supported by NSF, Harvard-MIT CUA and Packard and Sloan Foundations. Work at Yale is supported by NSF Grant DMR0325580, the W.M. Keck Foundation and the Army Research Office. Work at Innsbruck is supported by the Austrian Science Foundation, European Networks and the Institute for Quantum Information. J.M.D. would like to thank the Humboldt Foundation and G. Meijer for their support.
Correspondence and requests for materials should be addressed to M.D.L.

Competing financial interests

The authors declare that they have no competing financial interests.